Appl. Phys. A 76, 869–871 (2003)
DOI: 10.1007/s00339-002-1966-7

Applied Physics A
Materials Science & Processing

R. FRÖMTER[1,✉]
H.P. OEPEN[1]
J. KIRSCHNER[2]

A miniaturized detector for high-resolution SEMPA

[1] IAP, Universität Hamburg, Jungiusstraße 11, 20355 Hamburg, Germany
[2] MPI für Mikrostrukturphysik, Weinberg 2, 06120 Halle, Germany

Received: 2 September 2002/Accepted: 2 September 2002
Published online: 5 March 2003 • **© Springer-Verlag 2003**

ABSTRACT The basics of the scanning electron microscope with polarization analysis are briefly reviewed, emphasizing the achievable magnetic resolution and image contrast. The design of an optimized spin-polarization detector based on the well-established LEED scattering principle is presented. Results of first tests are reported.

PACS 07.78.+s; 07.77.Ka; 75.70.-i; 75.75.+a

1 Introduction

Scanning electron microscopy with polarization analysis (SEMPA) has developed into a powerful technique for the study of magnetic structures at surfaces and in ultrathin films. The technique is based on analyzing the spin polarization of secondary electrons created at the surface of itinerant ferromagnets by electrons. At very low secondary electron kinetic energies, an enhancement of the spin polarization is found, which is in the same energy range where the intensity has its maximum. Recognizing this very favorable condition, a new microscope was proposed to image magnetic domains [1, 2], and finally in 1984 the first SEMPA was realized [3]. The fundamental idea is to use the narrow primary beam of a scanning electron microscope (SEM) to create secondary electrons and analyze their spin polarization. Thus, the microscope consists of a SEM and an attached spin-polarization analyzer (Fig. 1).

The secondary electrons created at the sample (Fig. 1) are collected and focused into the spin analyzer via special electron optics. For the spin-polarization analysis, the electrons are scattered at a target. Different types of analyzers are used in SEMPA, such as the Mott detector [4, 5], the low-energy diffuse scattering detector [6], or the LEED (low-energy electron diffraction) detector [7]. Due to an extremely small depth of information of the spin polarization of the secondary electrons [8], the experiment has to be performed under ultra-high vacuum (UHV) conditions.

✉ Fax: +49-40/42838-6368,
E-mail: RFroemte@PHYSnet.Uni-Hamburg.de

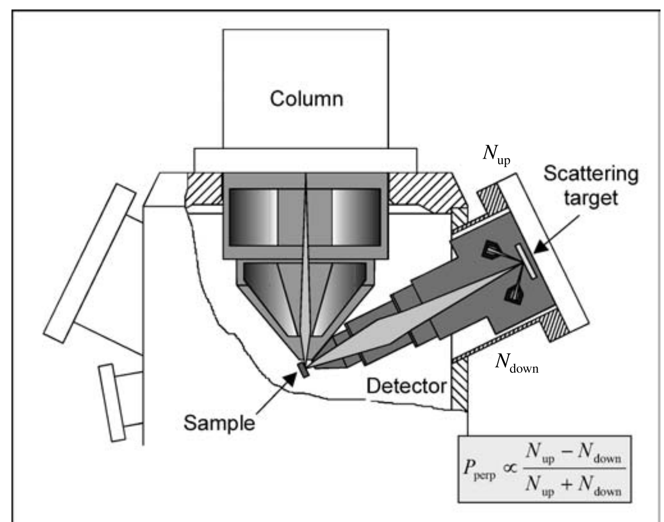

FIGURE 1 Sketch of SEMPA illustrating the relative orientation of SEM column, sample, and spin detector in the UHV chamber. One of the two orthogonal pairs of electron counters is shown in the drawing. The intensity asymmetry of the diffraction beams in opposite angles (upward N_{up} and downward N_{down}) is proportional to the component of the spin polarization, P_{perp}, perpendicular to the plane of the drawing. The short working distances of column and detector as well as the nearly perpendicular take-off angle are prerequisite to accomplishing ultra-high resolution (see text)

2 Theory

In principle, the diameter of the primary beam determines the spatial resolution of the technique. To be more precise, however, it turns out to be a combination of diameter and intensity of the primary beam that limits the imaging properties. To make that transparent, we will consider the contrast that can be achieved. The contrast in SEMPA is defined as

$$K = P/\delta P ,$$

with P the polarization signal and δP the statistical uncertainty of the polarization analysis [4, 6, 7]. In the electron-counting mode we obtain [9]

$$\delta P \approx 1/\sqrt{F\dot{N}t} ,$$

with F the figure of merit or efficiency of the detector $\dot{N}$, the number of electrons per second entering the detector and t the dwell time. Common to all the above-mentioned detectors is a very low efficiency, of the order of 10^{-4}. Due to this low figure of merit, the primary currents have to be high to keep the measurement time reasonably short. For a contrast $K \geq 2$ and a smallest detectable variation of polarization in the percent range, one needs primary currents in the range of nA to achieve an acceptable dwell time of 10 ms per pixel. Hence, microscopes with high primary currents are needed. Besides that, the achievable spin polarization, i.e. a property of the sample itself, is the most essential ingredient that determines the contrast.

In the beginning of SEMPA, such high SEM probe currents were at variance with a high spatial resolution [10] and there was no commercially available standard SEM column that incorporated these features into a UHV-compatible design. Special electron sources with high brightness were needed, like field-emission, or thermally-assisted field-(Schottky-) emission guns. Based on such a Schottky gun, a new SEMPA with a magnetic resolution of 5 nm has been realized recently [11]. There is an increasing demand in industry for ultra-high resolution (≤ 3 nm), UHV-compatible instruments with high primary-beam current. This interest, which stems from the ongoing strive for ever smaller structures in devices, is primarily biased towards chemical analysis (SAM, scanning auger microscopy). As a matter of fact, the prerequisites on the scanning electron beam are similar for SAM and SEMPA, which triggers new developments in magnetic nano-analysis as well. A new SEM/SAM column has been designed and optimized [12], which will be used in combination with the detector presented here. Recent performance tests with the new column have demonstrated that 4-nm resolution at a beam current of 1 nA can be achieved [13]. With these numbers, the realization of a new SEMPA with resolution better than 5 nm seems to become feasible.

3 The detector

From the technological point of view, there is a need for the combination of high-resolution SAM and SEMPA, particularly in the framework of worldwide spintronics activities. To meet the requirements of such an instrument, the spin detector should be compact, safe, and easy to operate while at the same time providing the highest magnetic contrast possible. As a detector, the LEED-type analyzer [14, 15] has been chosen, which utilizes electron scattering at a W(001) single-crystal surface to detect the spin polarization. The intensities of (2,0)-beams are compared, their normalized intensity difference being proportional to the polarization. Two perpendicular pairs of scattered beams can be used to measure two polarization components, simultaneously.

Since the LEED detector is operated at a kinetic energy of 104.5 V, no voluminous electrical insulation is necessary compared to, for example, a Mott detector. In the new design, four double microchannel plate (MCP) assemblies in chevron configuration have replaced the channeltron electron multipliers used in previous versions for electron counting (Fig. 2). The reason for this change is twofold: In the first place, the higher count rates caused by the "high-current" primary beam have to be mastered by the counting facilities and electronics. Therefore a sufficient pulse separation in the detector output signal has to be guaranteed. The pulse width at half maximum of our MCP system has been measured to be 5 ns while the pulse width of channeltron multipliers is typically 20 ns. In addition, due to the large number of individual channels in a MCP, the probability of striking the same channel twice in a row is minimal. Hence, the dead-time is in the range of the pulse duration, which makes 100-MHz counting feasible. Assuming the product of collection efficiency and secondary-electron yield to be unity and a scattering coefficient of 10^{-3} [15], a primary beam current of 1 nA will give a count rate of $6 \times 10^{6}\ \mathrm{s}^{-1}$ per scattering channel. This best-case estimate yields numbers that can easily be handled by our 100-MHz counting facility and electronics, even when taking into account that the scattering events have a Poisson-type distribution. Simultaneous data acquisition of all four intensity channels allows for online calculation of two orthogonal asymmetries, which represent the two orthogonal components of the magnetization vector.

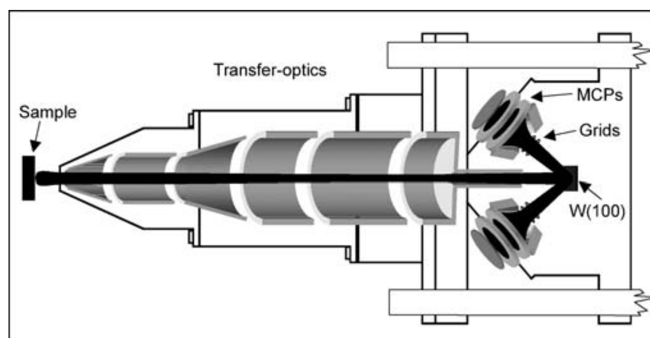

FIGURE 2 Schematic half-section of the spin detector. The transfer optics, which are designed to collect nearly all of the low-energy electrons emitted from the sample, consist of a stack of rotationally symmetric electrostatic tube lenses. The first and fourth elements are divided into four sectors to correct for beam misalignment and astigmatism. Two out of four microchannel plate assemblies are shown, which are used in electron-counting mode. The electron path shown is an approximation of the trajectories of low-energy electrons emitted into a 2π solid angle

A second advantage of using MCPs is the size of the MCP stack. The thickness is very small, which allows for a very compact design of the detector (Fig. 3). Consequently, the overall length of the system can be kept small, so that the whole detector and optics assembly can be positioned inside the main chamber. A detector chamber with separate pumping is no longer needed. The reduction of the detector size is limited essentially by the heating of the channel plates while flashing the W-crystal. In order to maintain spin sensitivity, flash cleaning cycles of the crystal are necessary at regular intervals during operation. Even though the crystal was chosen to be small ($6 \times 6\ \mathrm{mm}^2$), an electric power of 180 W had to be supplied via e-beam heating for some seconds to reach temperatures above 2000 K.

Figure 2 shows a schematic of the detector and optics. The optical system was positioned as close as possible to the sample, while the first elements were at high potential (typically 1.5 kV) to accelerate the electrons towards the detector. The optics and detector could be moved close to the sample via a linear feedthrough, with the smallest spacing from the front-

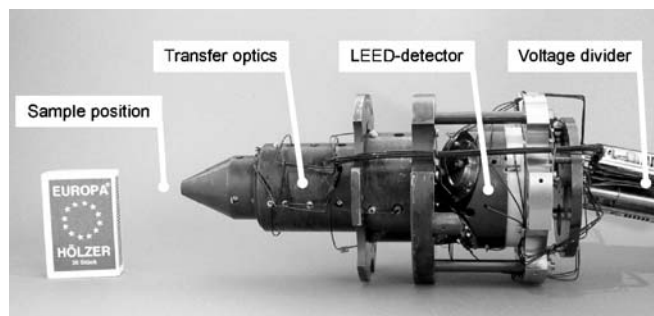

FIGURE 3 Photograph of the complete spin detector assembly. Note that the LEED detector is only slightly larger than the matchbox shown for comparison. Part of the four resistive voltage dividers can be seen on the right-hand side. The whole system is mounted on a base plate, which can be moved in and out by means of a linear feedthrough. This allows a working distance of 8 mm while operating and provides ample access for complementary surface-science techniques when retracted

end to the sample approximately 8 mm. A near-perpendicular take-off angle and the high voltage warranted a maximum solid angle of secondary electron collection. In particular, the lowest energy electrons with highest polarization were nearly completely focused into the detector. A collection efficiency of 80% was found for these electrons. The electron optics consisted of a consecutive assembly of six electrostatic tube elements, two of which were used as quadrupoles. The first two elements provided a strong acceleration. The following elements caused a controlled deceleration down to the scattering energy. After scattering at the W-crystal, the electrons had to pass two consecutive grids before being detected by a MCP. The first grid was held at the scattering potential. This assured a homogenous potential within the hemisphere surrounding the crystal, which was necessary for well-defined diffraction conditions. The second grid was a retarding grid used to filter out the inelastic background contribution.

All preliminary experiments with the newly designed detector performed so far are in good agreement with our design criteria. From this, we expect to meet the final resolution that has been proposed, i.e. the sub-10-nm range.

ACKNOWLEDGEMENTS Support by BMBF Grant No. 13N7484/5 is gratefully acknowledged.

REFERENCES

1 R.J. Celotta, D.T. Pierce: In: *Microbeam Analysis*, ed. by K.F.J. Heinrich (San Francisco Press, San Francisco 1982) p. 469
2 J. Kirschner: Scanning Electron Microsc. **III**, 1179 (1984)
3 K. Koike, K. Hayakawa: Jpn. J. Appl. Phys. **23**, L187 (1984)
4 K. Koike, H. Matsuyama, K. Hayakawa: Scanning Microsc. Intern. Suppl. **1**, 241 (1987)
5 R. Allenspach: IBM J. Res. Develop. **44**, 553 (2000)
6 G.G. Hembree, J. Unguris, R.J. Celotta, D.T. Pierce: Scanning Microsc. Intern. Suppl. **1**, 229 (1987)
7 H.P. Oepen, J. Kirschner: Scanning Microsc. **5**, 1 (1991)
8 D.L. Abraham, H. Hopster: Phys. Rev. Lett. **58**, 1352 (1987)
9 J. Kessler: *Polarized Electrons*, 2nd edn. (Springer, Berlin 1985)
10 L. Reimer: *Scanning Electron Microscopy: Physics of Image Formation and Microanalysis* (Springer, Berlin 1985)
11 T. Kohashi, K. Koike: Jpn. J. Appl. Phys. **40**, L1264 (2001)
12 UHV-Gemini column, developed by a cooperation of: OMICRON NanoTechnology GmbH, Taunusstein, Germany, LEO Elektronenmikroskopie GmbH, Oberkochen, Germany, CEOS GmbH, Heidelberg, Germany
13 J. Westermann, private communication; see also http://www.omicron.de/nano/
14 J. Kirschner, R. Feder: Phys. Rev. Lett. **42**, 1008 (1979)
15 J. Kirschner: *Polarized Electrons at Surfaces*, 2nd edn. (Springer, Berlin 1985)